An Endohedral Single-Molecule Magnet with Long Relaxation Times: DySc2N@C80

— **Source link** ⧉

Rasmus Westerström, Jan Dreiser, Cinthia Piamonteze, Matthias Muntwiler ...+9 more authors

Institutions: University of Zurich, Paul Scherrer Institute, École Polytechnique Fédérale de Lausanne, Leibniz Association ...+1 more institutions

Topics: SQUID, Relaxation (NMR), Single-molecule magnet, Magnetism and Magnetic circular dichroism

Related papers:

- Lanthanide Double-Decker Complexes Functioning as Magnets at the Single-Molecular Level

- Tunneling, remanence, and frustration in dysprosium-based endohedral single-molecule magnets

- Magnetic bistability in a metal-ion cluster

- Exploiting single-ion anisotropy in the design of f-element single-molecule magnets

- Lanthanide single-molecule magnets.

Year: 2012

An endohedral single-molecule magnet with long relaxation times: DySc2N@C80

Westerström, Rasmus ; Dreiser, Jan ; Piamonteze, Cinthia ; Muntwiler, Matthias ; Weyeneth, Stephen ; Brune, Harald ; Rusponi, Stefano ; Nolting, Frithjof ; Popov, Alexey ; Yang, Shangfeng ; Dunsch, Lothar ; Greber, Thomas

Abstract: The magnetism of DySc2N@C80 endofullerene was studied with X-ray magnetic circular dichroism (XMCD) and a magnetometer with a superconducting quantum interference device (SQUID) down to temperatures of 2 K and in fields up to 7 T. XMCD shows hysteresis of the 4f spin and orbital moment in DyIII ions. SQUID magnetometry indicates hysteresis below 6 K, while thermal and nonthermal relaxation is observed. Dilution of DySc2N@C80 samples with C60 increases the zero-field 4f electron relaxation time at 2 K to several hours.

DOI: https://doi.org/10.1021/ja301044p

An endohedral single-molecule magnet with long relaxation times: $DySc_2N@C_{80}$

Rasmus Westerström,[†,‡] Jan Dreiser,[‡] Cinthia Piamonteze,[‡] Matthias Muntwiler,[‡] Stephen Weyeneth,[†] Harald Brune,[¶] Stefano Rusponi,[¶] Frithjof Nolting,[‡] Alexey Popov,[§] Shangfeng Yang,[§,‖] Lothar Dunsch,[§] and Thomas Greber*,[†]

Physik-Institut, Universität Zürich, Winterthurerstrasse 190, CH-8057 Zürich, Switzerland, Swiss Light Source, Paul Scherrer Institut, CH-5232 Villigen PSI, Switzerland, Institute of Condensed Matter Physics, Ecole Polytechnique Fédérale de Lausanne, CH-1015 Lausanne, Switzerland, Department of Electrochemistry and Conducting Polymers, Leibniz Institute of Solid State and Materials Research, Dresden, D-01069 Dresden, Germany, and Hefei National Laboratory for Physical Sciences at Microscale, Department of Materials Science and Engineering, University of Science and Technology of China, 96 Jinzhai Road, Hefei 230026, China

Received May 11, 2012; E-mail: greber@physik.uzh.ch

Abstract: The magnetism of $DySc_2N@C_{80}$ endofullerene samples was studied with x-ray magnetic circular dichroism (XMCD) and a magnetometer equipped with a superconducting quantum interference device (SQUID) down to temperatures of 2 K and in fields up to 7 T. XMCD shows hysteresis of the $4f$ spin and orbital moment in Dy^{III} ions. SQUID magnetometry indicates as well hysteresis below 6 K, while thermal and non-thermal relaxation is observed. Dilution of $DySc_2N@C_{80}$ samples with C_{60} increases the zero field $4f$ electron relaxation time at 2 K to several hours.

Incorporation of magnetic ions in molecular clusters can lead to the formation of so-called single-molecule magnets (SMMs).[1–6] These molecules are characterized by a slow magnetic relaxation, making them candidates for future applications in quantum computing, spintronics, and high-density storage devices.[7,8]

Mononuclear complexes exhibiting SMM behavior were first demonstrated for the double-decker phthalocyanines, $[Pc_2Ln^{III}]^-$ (Ln^{III}=Tb,[9,10] Dy,[9,10] or Ho[11]). To date, the class of mononuclear SMMs has been extended with other lanthanide complexes,[12–21] and recently it was shown that mononuclear complexes of actinides[22–24] and first-row transition metals[25,26] can exhibit SMM behavior.

Also dinuclear dysprosium complexes show distinct SMM behaviour,[27–30] though the present communication deals with slow magnetisation dynamics in the mononuclear dysprosium complex $DySc_2N@C_{80}$.

The magnetism in lanthanide complexes is somewhat different from their transition-metal counterparts. The $4f$ levels of lanthanide ions have an unquenched orbital moment and a $(2J+1)$-fold degenerate ground state. If this degeneracy is lifted in a ligand field (LF), different J_z states can be separated by an energy comparable to the thermal energy at room temperature.[17]

Metal nitride clusterfullerenes (NCFs) offer the opportunity to encage up to 3 paramagnetic ions. Since their first isolation[31] they found a widespread interest in research.[32–34] Variation of the 3 metal ions implies a great diversity of the endohedral units like $M_xSc_{3-x}N@C_{80}$ (x = 1, 2, M = Er,[35,36] Gd,[37,38] Y,[39] Lu[40]), $TbSc_2N@C_{80}$,[41] $CeSc_2N@C_{80}$,[42] $Lu_2CeN@C_{80}$, $NdSc_2N@C_{80}$,[40] $DySc_2N@C_{76}$,[43] $DySc_2N@C_{68}$,[44] $Lu_xSc_{3-x}N@C_{68}$ (x = 1-2),[44] $ScYErN@C_{80}$,[45] $Lu_xY_{3-x}N@C_{80}$ (x = 1, 2),[46] $TiSc_2N@C_{80}$.[47]

Investigations on the magnetism of single ions inside fullerenes started with $Gd@C_{82}$, which turned out to be paramagnetic down to a temperature of 3 K.[48] Also for $Dy@C_{82}$ SQUID and XMCD revealed a paramagnetic behavior down to 1.8 K.[49–52] In this system, the observed magnetic moment is reduced compared to the free trivalent Dy ion. This effect has been attributed to a quenched orbital moment due to the crystal field splitting from the carbon cage and/or an electron back donation from the cage to the Dy ion. In contrast, the C_{80} NCFs have a carbon cage with a closed shell, and less coupling between the moments of the metal ions and a diamagnetic cage is expected. Instead, the magnetic properties are to a large extent governed by the central N^{3-} ion. SQUID magnetization measurements performed on $Ln_3N@C_{80}$ (Ln=Tb and Ho)[53,54] are in line with a model where the ligand field of the N^{3-} ion induces an easy axis for the individual Ln^{III} moments directed along the respective Ln-N bond. In this model the magnetic anisotropy due to the ligand field is strong enough, such that the Ln^{III} moments do not align to the external field, but instead parallel to the bond directions, which explains the reduced net magnetic moment of the Ln_3N trimer.[53] Nevertheless, the magnetization curves recorded on $Ln_3N@C_{80}$ (Ln = Tb,[53,54] Ho,[53,54] Tm,[55] Er,[56,57] Gd[58]) and $Er_xSc_{3-x}N@C_{80}$[56] (x = 1, 2), at temperatures above 1.8 K showed paramagnetism without hysteresis.

In the present case we have a single Dy^{III} ion in a diamagnetic carbon cage. Since Sc^{III} ions are not paramagnetic, the ligand field due to the N^{3-} ion will result in a magnetic anisotropy directed along the Dy-N bond. Furthermore, if the LF stabilizes a ground state with a large J_z, the prerequisite for magnetic bistability is fulfilled.

The robustness of endofullerene molecules and their ordering on surfaces[59] makes them ideal model systems for studying and possibly exploiting the intrinsic magnetic properties of SMMs deposited on substrates. Here we show that the $DySc_2N@C_{80}$ endofullerene exhibits SMM behavior with long relaxation times. By combining element specific x-ray magnetic circular dichroism (XMCD)[60–62] and superconducting quantum interference device (SQUID) magnetometry on diluted an non-diluted samples, it is demonstrated that the magnetic behavior of $DySc_2N@C_{80}$ can be attributed to single Dy^{III} ions.

The $DySc_2N@C_{80}$ (isomer I_h, see Figure 1) was produced by a modified Krätschmer-Huffman dc-arc discharge method in a mixture of NH_3 (20 mbar) and He (200 mbar) atmosphere as described elsewhere.[36,43] Briefly, a mixture of naturally abundant Dy_2O_3 and Sc_2O_3 (99.9%, MaTeck GmbH, Germany) with graphite powder was used (molar ratio Dy:Sc:C=1:1:15). After dc-arc discharge

[†]Universität Zürich

[‡]Paul Scherrer Institut

[¶]Ecole Polytechnique Fédérale de Lausanne

[§]Leibniz Institute of Solid State and Materials Research
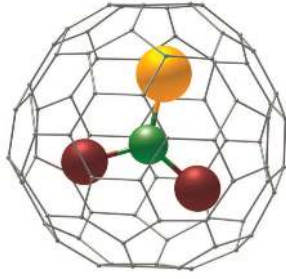
[‖]University of Science and Technology of China

Figure 1. Chemical structure of $DySc_2N@C_{80}$, Green = N, dark purple = Sc, Orange = Dy. The C_{80} cage is shown as a wire frame.

treatment, the soot was pre-extracted using acetone and further Soxhlet-extracted using CS_2 for 20 h. Fullerene isolation was performed by three-step HPLC. In the first step running in a HP instrument (series 1100) a combination of two analytical 4.6 × 250 mm Buckyprep columns (Nacalai Tesque, Japan) was applied with toluene as the eluent. The second and third-step isolations were performed by recycling HPLC (Sunchrom, Germany) using a semi-preparative 4.6 × 250 mm 5PYE or Buckyprep-M column (Nacalai Tesque, Japan) and toluene as the eluent. An UV detector set to 320 nm was used for fullerene detection in all separations. The purity of the final samples was checked by laser desorption time-of-flight (LD-TOF) mass spectrometry both in positive and negative ion modes (Biflex III, Bruker, Germany). The $DySc_2N@C_{80}$ compounds are characterized by UV-Vis-NIR and FTIR spectroscopy.[40]

The x-ray absorption experiments were performed at the X-Treme beamline at the Swiss Light Source, Paul Scherrer Institut, Villigen, Switzerland, in fields up to 7 T along the beam direction and temperatures down to 2 K.[63] The molecules were drop cast from a toluene solution onto a polycrystalline aluminum sample plate. The samples were cooled in zero field from RT down to $\sim$ 2 K. The absorption was measured by recording the total electron yield normalized with the photon flux.

The SQUID measurements were performed using undiluted samples (**1**) and a sample diluted with C_{60} (**2**). The net mass of the samples is in the μg range. The diluted sample was prepared by mixing two toluene solutions, one containing C60 and one containing DySc2N@C80, with volume ratio of 10:1. Taking into account the difference in solubility between the two molecules yields a final molar ratio between 10:1 and 20:1. To ensure a low background signal for the SQUID measurements, the molecules were drop cast onto a sample holder made from kapton foil with a mass of $\sim$ 10 mg. Before molecule deposition, the sample holders were characterized at different magnetic fields and temperatures. The sample holders for the present experiments exhibited a weak linear diamagnetic behavior. This diamagnetic background has been subtracted. The history of the samples is the same as for those used in the XMCD measurements, cooling from room temperature (RT) to 2 K took place in zero field. All magnetization versus field measurements were started at +7 T, and the magnetization loop was recorded within ±7 T at an average field sweep rate of 1.3 mTs^{-1}.

Figure 2 (a) displays the x-ray absorption in the energy range of the Dy $M_{4,5}$-edges, where the data are normalized with the maximum $3d \rightarrow 4f$ absorption signal of right and left circular polarized light $(I^+ + I^-)$. The spectra were recorded on sample **1** with the temperature set to 2 K and a magnetic field of 6 T. The polarization-dependent x-ray absorption spectra after background subtraction I^+ and I^- and the resulting XMCD spectrum $I^+ - I^-$, are shown in the middle and bottom panel of Figure 2 (a). Using the sum rules,[64,65]
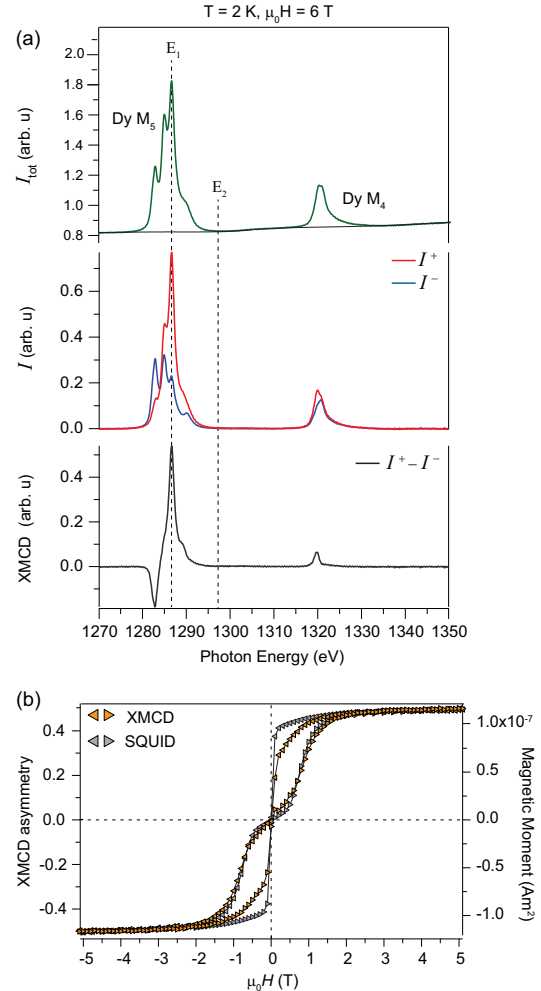

Figure 2. sample **1** (a) Top panel: Sum of the x-ray absorption spectra of both x-ray helicities I_{tot} recorded at the Dy $M_{4,5}$-edge at 6 T. Center panel: Polarization dependent x-ray absorption spectra after subtraction of the background, I^+ (red) and I^- (blue). Bottom panel: Magnetic-circular-dichroism XMCD $(I^+ - I^-)$. (b) Magnetization curves recorded by XMCD and SQUID magnetometry at 2 K. The element-specific magnetization curve was measured at the Dy M_5-edge by recording the total yield at photon energies E_1 and E_2 in panel (a) using a fixed photon helicity, while the magnetic field was ramped from +6 T to -6 T and back again. After changing the beam helicity the measurement was repeated and the magnetization curve was constructed from the assymmetry $[(I_{E_1}^+ - I_{E_2}^+) - (I_{E_1}^- - I_{E_2}^-)]/[(I_{E_1}^+ - I_{E_2}^+) + (I_{E_1}^- - I_{E_2}^-)]$.

the average magnetic moment of the Dy^{III} ions was extracted from the dichroism and the total absorption spectra in Figure 2 (a). From the calculation we obtain a ratio of $\langle L_z \rangle / \langle S_z \rangle = 1.75$, in good agreement with the value of 2 derived from a $4f^9$ occupancy and Hund's rules, which predict a $^6H_{15/2}$ groundstate. The expectation value of the Dy $\langle T_z \rangle$ operator was evaluated analytically according to eq. 8 in ref.[65] At saturation, the average Dy^{III} magnetic moment gets $m_{sat} = 4.4\ \mu_B$. This value is lower than $15/2 \cdot g_J \mu_B = 10\ \mu_B$ as expected from the Hund ground state with a Landé factor $g_J = 20/15$, even if it is reduced by a factor of $1/2$ due to an isotropic distribution of the easy axes.[66] In the present case, the ligand field could stabilize a ground state different from $J_z = \pm 15/2$, explaining the additional reduction of the observed magnetic moment.

Figure 2 (b) displays the element-specific magnetization curve obtained from XMCD at the Dy M_5-edge, together with the field dependence of the total magnetic moment measured by SQUID magnetometry. The agreement between the two data sets demonstrates that the magnetic moments measured by our SQUID magnetometer can be attributed to the Dy^{III} ions. From the observed hysteresis loops it is evident that the system exhibits slow magnetic relaxation. The shape of the hysteresis will depend on the relaxation rate, and consequently, the deviation between the two data sets may be caused by a slightly higher sample temperature during the XMCD measurement and different field scan rates for the two experiments of 1.3 mTs^{-1} (SQUID) and 17 mTs^{-1} for (XMCD), respectively.

Magnetization loops from **1** recorded at different temperatures using SQUID magnetometry are shown in Figure 3. Below 6 K hysteresis is observed. A hysteresis was also detected in the temperature range 2 K$\leq T < 5$ K for sample **2** diluted with 10-20 times C$_{60}$, indicating that the magnetic bistability is a property of the single Dy^{III} ions, rather than due to intermolecular magnetic interactions.
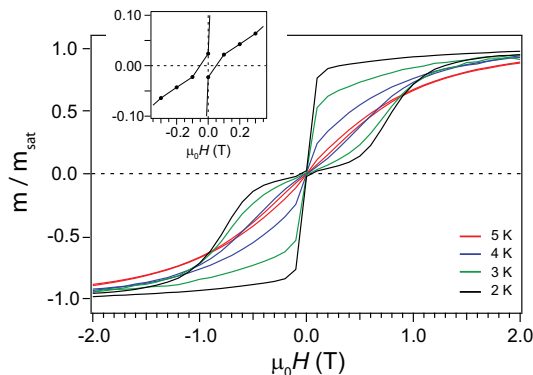

Figure 3. Temperature dependent magnetization curves for sample **1** recorded using SQUID magnetometry. The inset shows an enlargement of the 2 K signal at small fields. m_{sat} is the saturated magnetization measured at 7 T.

Hysteresis curves with sharp drops at low fields have been reported for other single molecule magnets such as [Pc$_2$Dy]$^-$ [67] or (Cp*)Er(COT).[17] They depend not only on temperature but also on scan time, which indicates that we deal here with slow magnetization dynamics rather than with the hysteresis of a ferromagnet: The magnetization relaxes to an equilibrium, which depends on field and temperature. This was further investigated by time dependent SQUID measurements. Figure 4 (a) shows three relaxation curves at 2 K. At $t = 0$ the field was switched from 0.4 T to 0.3 T (0.5 T to 0 T), after being ramped down from 7 T at an average speed of 5.4 mTs^{-1} (4.5 mTs^{-1}). Below 3.5 K relaxation data do not exhibit a simple exponential decay, which indicates more than one relaxation

process. In this temperature range, a double exponential

$$m(t) = m(t \to \infty) + \alpha \exp(-t/\tau_A) + \beta \exp(-t/\tau_B);\ \ \tau_A > \tau_B,\ \ (1)$$

was fitted to the magnetization curves $m(t)$, where the data were weighted with the noise. α and β are the magnetization of relaxation process A and B at $t = 0$, and τ_A and τ_B the corresponding relaxation times. Above 3.5 K, a single exponential, $\alpha \exp(-t/\tau_A)$, was used for fitting the $m(t)$ curves.

The resulting decay times for the slower process, τ_A, are displayed as a function of inverse temperature in Figure 4 (b). As expected for a thermally activated process, the relaxation times decrease with temperature.

Thermal relaxation mechanisms are generally attributed to higher order phonon processes, such as e.g. the Orbach process between the J_z levels. In order to estimate the effective barrier for thermally driven relaxation, Δ_{eff}, the function

$$\tau(T) = \frac{\tau_c \cdot \tau_0 \exp(\Delta_{eff}/k_BT)}{\tau_c + \tau_0 \exp(\Delta_{eff}/k_BT)} \quad (2)$$

was fitted to the relaxation times. τ_c is the temperature independent decay time, and τ_0 the exponential prefactor for the temperature dependent part. For sample (**1**) at 0.3 T we obtain a value of $\Delta_{eff}/k_B = 24 \pm 0.5$ K, which compares to 21.7 K of [Pc$_2$Dy]$^-$ (at 350 μT ac). On the other hand, the exponential prefactor has an exceptionally large value, $\tau_0 = 1 \pm 0.1$ s, which is more than four orders of magnitude larger than that of [Pc$_2$Dy]$^-$.[10] This indicates peculiar magnetization dynamics in the present system. In contrast to molecules such as [Pc$_2$Dy]$^-$, the magnetic moments are in the DySc$_2$N@C$_{80}$ endofullerene protected by a diamagnetic cage and a low phonon density may inhibit thermal relaxation.

The temperature independent decay times τ_c^A and τ_c^B get $\sim 10^4$ and $\sim 8 \times 10^2$ s, respectively. The τ_c's are ascribed to magnetization decay through quantum tunneling between the $\pm J_z$ states. Since the Dy^{III} ion contains an odd number of electrons, all states have a double degeneracy according to Kramer's theorem. In this case, quantum tunneling is only possible in the presence of a perturbation which lifts the degeneracy and allows the doublets to mix. In the present system, Zeeman splitting, intermolecular dipole-dipole or hyperfine interaction with the nuclear spin may give rise to such a perturbation.

The relaxation time in zero field is of particular interest since it is the 'remanence time' for a given sample. In zero field there is no Zeeman splitting and intermolecular dipole-dipole interaction, which must be small due to the protection of the Dy by the C$_{80}$ cage, can be further weakened in increasing the distance between the Dy atoms. This was achieved by diluting the sample with C$_{60}$. The data points of sample (**2**) in Figure 4 show that dilution leads to a significant increase of the relaxation time at 0 T and 2 K. The relaxation time for sample (**2**), $\tau_A^{(2)}$ in zero field is now > 5 h, which is about nine times longer than that for undiluted samples ($\tau_A^{(1)} \sim 40$ min). The ratio τ_B/τ_A is ~ 0.2, and $\alpha/\beta \sim 1$, for both, (**1**) and (**2**). If the two relaxation processes A and B are affected equally by intermolecular dipole-dipole interactions, this could be a hint that the difference between A and B is due to different Dy isotopes, i.e. hyperfine interactions between the J_z level and the corresponding nuclear spin.

At 4 K and 0.3 T, samples (**1**) and (**2**) exhibit the same relaxation times (within 10%), as expected for thermally driven magnetic relaxation of individual molecules.

In summary, DySc$_2$N@C$_{80}$ has been shown to be a mononuclear single-molecule magnet with a hysteresis below 6 K. The magnetic moment is attributed to the Dy^{III} ion in the diamagnetic carbon cage and the $4f$ electrons display exceptionally long relaxation times. If the sample is diluted the relaxation of the magnetization at 2 K

increases by a factor of nine.

Supporting information: Full author list of ref.[66]

References

(1) Caneschi, A.; Gatteschi, R., Dand Sessoli; Barra, A. L.; Brunel, L.; Guillot, M. J. *J. Am. Chem. Soc.* **1991**, *113*, 5873.
(2) Sessoli, R.; Tsai, H.-L.; Schake, A. R.; Wang, S.; Vincent, J. B.; Folting, K.; Gatteschi, D.; Christou, G.; Hendrickson, D. N. *J. Am.Chem. Soc.* **1993**, *115*, 1804–1816.
(3) Sessoli, R.; Gatteschi, D.; Caneschi, A.; Novak, M. *Nature* **1993**, *365*, 141–143.
(4) Friedman, J. R.; Sarachik, M. P.; Tejada, J.; Ziolo, R. *Phys. Rev. Lett.* **1996**, *76*, 3830.
(5) Christou, G.; Gatteschi, D.; Hendrickson, D. N.; Sessoli, R. *MRS Bull* **2000**, *25*, 66.
(6) Cadiou, C.; Murrie, M.; Paulsen, C.; Villar, V.; Wernsdorfer, W.; Winpenny, R. E. P. *Chem. Commun* **2001**, *2666*.
(7) Leuenberger, M. N.; Loss, D. *Nature* **2001**, *410*, 789–793.
(8) Bogani, L.; Wernsdorfer, W. *Nat Mater* **2008**, *7*, 179–186.
(9) Ishikawa, N.; Sugita, M.; Ishikawa, T.; Koshihara, S.-y.; Kaizu, Y. *J. Am.Chem. Soc.* **2003**, *125*, 8694–8695.
(10) Ishikawa, N.; Sugita, M.; Ishikawa, T.; Koshihara, S.-y.; Kaizu, Y. *J. Phys. Chem. B.* **2004**, *108*, 11265–11271.
(11) Ishikawa, N.; Sugita, M.; Wernsdorfer, W. *J. Am.Chem. Soc.* **2005**, *127*, 3650–3651.
(12) AlDamen, M. A.; Clemente-Juan, J. M.; Coronado, E.; Martí-Gastaldo, C.; no, A. G.-A. *J. Am. Chem. Soc.* **2008**, *130*, 8874–8875.
(13) AlDamen, M. A.; Cardona-Serra, S.; Clemente-Juan, J. M.; Coronado, E.; Gaita-Arin, A.; Martĺ-Gastaldo, C.; Luis, F.; Montero, O. *Inorg. Chem.* **2009**, *48*, 3467–3479.
(14) Li, D.-P.; Wang, T.-W.; Li, C.-H.; Liu, D.-S.; Li, Y.-Z.; You, X.-Z. *Chem. Commun.* **2010**, *46*, 2929.
(15) Jiang, S.-D.; Wang, B.-W.; Su, G.; Wang, Z.-M.; Gao, S. *Angew. Chem. Int. Ed.* **2010**, *49*, 7448.
(16) Gonidec, M.; Luis, F.; Vílchez, A.; Esquena, J.; Amabilino, D.; Veciana, J. A. *Angewandte Chemie* **2010**, *122*, 1667–1670.
(17) Jiang, S.-D.; Wang, B.-W.; Sun, H.-L.; Wang, Z.-M.; Gao, S. *J. Am. Chem. Soc.* **2011**, *133*, 4730–4733.
(18) Watanabe, A.; Yamashita, A.; Nakano, M.; Yamamura, T.; Kajiwara, T. *Chem. Eur. J* **2011**, *17*, 7428–7432.
(19) Car, P.-E.; Perfetti, M.; Mannini, M.; Favre, A.; Caneschi, A.; Sessoli, R. *J. Am. Chem. Soc* **2011**, *47*, 3751–3753.
(20) Jeletic, M.; Lin, P.-H.; J. Le Roy, J.; Korobkovand, I.; Gorelsky, S. I.; Murugesu, M. *J. Am. Chem. Soc.* **2011**, *133*, 19286–19289.
(21) Jiang, S.-D.; Liu, S.-S.; Zhou, L.-N.; Wang, B.-W.; Wang, Z.-M.; Gao, S. *Inorg. Chem.* **2012**, *51*, 3079–3087.
(22) Rinehart, J. D.; Long, J. R. *J. Am. Chem. Soc.* **2009**, *131*, 12558–12559.
(23) Antunes, M. A.; Pereira, L. C. J.; Santos, I. C.; Mazzanti, M.; Marc-alo, J.; Almeida, M. *Inorg. Chem.* **2011**, *50*, 9915–9917.
(24) Magnani, N.; Apostolidis, C.; Morgenstern, A.; Colineau, E.; Griveau, J.-C.; Bolvin, H.; Walter, O.; Caciuffo, R. *Angew. Chem. Int. Ed* **2011**, *50*, 1696.
(25) Freedman, D. E.; Harman, W. H.; Harris, T. D.; Long, G. J.; Chang, C. J.; Long, J. R. *J. Am. Chem. Soc* **2010**, *132*, 1224–1225.
(26) Zadrozny, J. M.; Long, J. R. *J. Am. Chem.Soc.* **2011**, *133*, 20732–20734.
(27) Long, J.; Habib, F.; Lin, P.-H.; Korobkov, I.; Enright, G.; Ungur, L.; Wernsdorfer, W.; Chibotaru, L. F.; Murugesu, M. *J. Am. Chem. Soc* **2011**, *133*, 5319–5328.
(28) Habib, F.; Lin, P.-H.; Long, J.; Korobkov, I.; Wernsdorfer, W.; Murugesu, M. *J. Am. Chem. Soc* **2011**, *133*, 8830–8833.
(29) Guo, Y.-N.; Xu, G.-F.; Wernsdorfer, W.; Ungur, L.; Guo, Y.; Tang, J.; Zhang, H.-J.; Chibotaru, L. F.; Powell, A. K. *J. Am. Chem. Soc* **2011**, *133*, 11948–11951.
(30) Lin, P.-H.; Sun, W.-B.; Yu, M.-F.; Li, G.-M.; Yan, P.-F.; Murugesu, M. *J. Am. Chem. Soc* **2011**, *47*, 10993–10995.
(31) Stevenson, S.; Rice, G.; Glass, T.; Harich, K.; Cromer, F.; Jordan, M.; Craft, J.; Hadju, E.; Bible, R.; Olmstead, M.; Maitra, K.; Fisher, A.; Balch, A.; Dorn, H. *Nature* **1999**, *401*, 55–57.
(32) Dunsch, L.; Yang, S. F. *Phys. Chem. Chem. Phys* **2007**, *9*, 3067–3081.
(33) Dunsch, L.; Yang, S. F. *Small* **2007**, *3*, 1298–1320.
(34) Chaur, M. N.; Melin, F.; Ortiz, A. L.; Echegoyen, L. *Angew. Chem.-Int. Edit* **2009**, *48*, 7514–7538.
(35) Olmstead, M. M.; de Bettencourt-Dias, A.; Duchamp, J. C.; S. Stevenson, H. C., Dorn; Balch, A. L. *J. Am. Chem. Soc* **2000**, *122*, 12220–12226.
(36) Dunsch, L.; Krause, M.; Noack, J.; Georgi, P. *J. Phys. Chem. Solids* **2004**, *65*, 309–315.
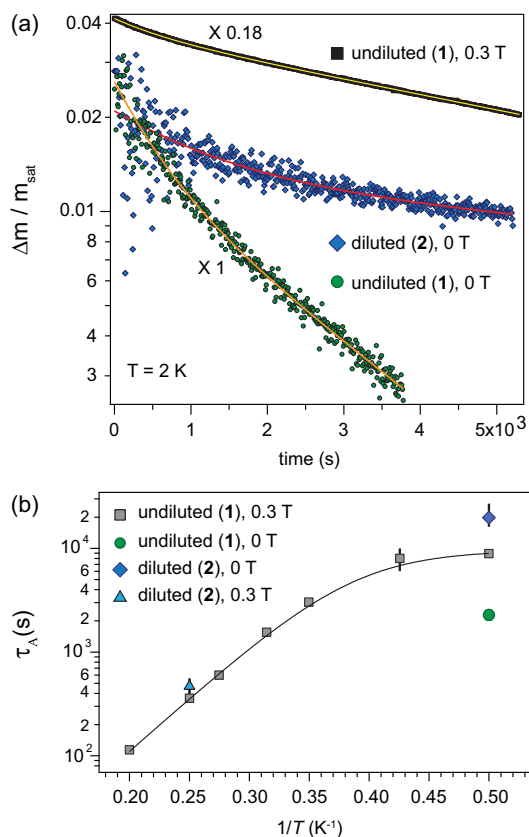(37) Yang, S. F.; Kalbac, M.; Popov, A.; Dunsch, L. *ChemPhysChem* **2006**, *71990-1995*.

Figure 4. (a) Temperature dependent magnetization for sample **1** and **2** at $T = 2$ K, with $\Delta m(t) = m(t) - m(t \rightarrow \infty)$. m_{sat} is the saturation magnetization. The lines correspond to the best fit of a double exponential Eq. (1). (b) The magnetic relaxation time τ_A as a function of inverse temperature. The three data points at $1/T = 0.5$ K^{-1} correspond to the relaxation times from the data in (a). The decay times at 0.3 T for the undiluted sample were fitted to the function in Eq. (2) (solid line).

(38) Yang, S. F.; Popov, A. A.; Kalbac, M.; Dunsch, L. *Chem.-Eur. J* **2008**, *14*, 2084–2092.

(39) Chen, N.; Fan, L. Z.; Tan, K.; Shu, Y. Q. W. C. Y.; Lu, X.; Wang, C. R. *J. Phys. Chem. C* **2007**, *111*, 11823–11828.

(40) Yang, S.; Popov, A. A.; Chen, C.; Dunsch, L. *J. Phys. Chem. C* **2009**, *113*, 7616–7623.

(41) Stevenson, S.; Chancellor, C.; Lee, H. M.; Olmstead, M. H.; Balch, A. L. *Inorg. Chem* **2008**, *47*, 1420–1427.

(42) Wang, X. L.; Zuo, T. M.; Olmstead, M. M.; Duchamp, J. C.; Glass, T. E.; Cromer, F.; Balch, A. L.; Dorn, H. C. *J. Am. Chem. Soc* **2006**, *128*, 8884–8889.

(43) Yang, S.; Popov, A. A.; Dunsch, L. *J. Phys. Chem. B* **2007**, *111*, 13659–13663.

(44) Yang, S. F.; Popov, A. A.; Dunsch, L. *Chem. Commun.* **2008**, 2885–2887.

(45) Chen, N.; Zhang, E. Y.; Wang, C. R. *J.Phys.Chem.B* **2006**, *110*, 13322–13325.

(46) Yang, S.; Popov, A. A.; Dunsch, L. *Angew. Chem.-Int. Edit. Engl* **2008**, *47*, 8196–8200.

(47) Yang, S.; Chen, C.; Popov, A.; Zhang, W.; Liu, F.; Dunsch, L. *Chem. Commun* **2009**, 6391–6393.

(48) Funasaka, H.; Sakurai, K.; Oda, Y.; Yamamoto, K.; Takahashi, T. *Chemical Physics Letters* **1995**, *232*, 273 – 277.

(49) Huang, H. J.; Yang, S. H.; Zhang, X. X. *J. Phys. Chem. B* **2000**, *104*, 1473–1482.

(50) De Nadai, C.; Mirone, A.; Dhesi, S. S.; Bencok, P.; Brookes, N. B.; Marenne, I.; Rudolf, P.; Tagmatarchis, N.; Shinohara, H.; Dennis, T. J. S. *Phys. Rev. B* **2004**, *69*, 7.

(51) Bondino, F.; Cepek, C.; Tagmatarchis, N.; Prato, M.; Shinohara, H.; Goldoni, A. *J. Phys. Chem. B* **2006**, *110*, 7289–7295.

(52) Kitaura, R.; Okimoto, H.; Shinohara, H.; Nakamura, T.; Osawa, H. *Phys. Rev. B* **2007**, *76*, 172409.

(53) Wolf, M.; Müller, K.-H.; Skourski, Y.; Eckert, D.; Georgi, P.; Krause, M.; Dunsch, L. *Angew. Chem. Int. Ed.* **2005**, *44*, 3306.

(54) Wolf, M.; K.-H. Müller, D. E.; Skourski, Y.; Georgi, P.; Marczak, R.; Krause, M.; Dunsch, L. *J. Magn. Magn. Mater.* **2005**, *290*, 290–293.

(55) Zuo, T.; Olmstead, M. M.; Beavers, C. M.; Balch, A. L.; Wang, G.; Yee, G. T.; Shu, C.; Xu, L.; Elliott, B.; Echegoyen, L.; Duchamp, J. C.; Dorn, H. C. *Inorg. Chem.* **2008**, *47*, 5234–5244.

(56) Tiwari, A.; Dantelle, G.; Porfyrakis, K.; Watt, A. A. R.; Ardavan, A.; Briggs, G. A. D. *Chem. Phys. Lett* **2008**, *466*, 155–158.

(57) Smirnova, T. I.; Smirnov, A. I.; Chadwick, T. G.; Walker, K. L. *Chem. Phys. Lett* **2008**, *453*, 233–237.

(58) Chen, L.; Carpenter, E. E.; Hellberg, C. S.; Dorn, H. C.; Shultz, M.; Wernsdorfer, W.; Chiorescu, I. *J. Appl. Phys* **2011**, *109*, 07B101–103.

(59) Treier, M.; Ruffieux, P.; Fasel, R.; Nolting, F.; Yang, S.; Dunsch, L.; Greber, T. *Phys. Rev. B* **2009**, *80*, 081403.

(60) van der Laan, G.; Thole, B. T. *Phys. Rev. B* **1991**, *43*, 13401.

(61) Stöhr, J. *J. Magn. Magn. Mater* **1999**, *200*, 470.

(62) Funk, T.; Deb, A.; George, S. J.; Wang, H.; Cramer, S. P. *Coord. Chem. Rev.* **2005**, *249*, 3.

(63) Piamonteze, C.; Flechsig, U.; Rusponi, S.; Dreiser, J.; Heidler, J.; Schmidt, M.; Wetter, R.; Schmidt, T.; Pruchova, H.; Krempasky, J.; Quitmann, C.; Brune, H.; Nolting, F. *In preparation*

(64) Thole, B. T.; Carra, P.; Sette, F.; Laan, G. v. d. *Phys. Rev. Lett* **1992**, *68*, 1943–1946.

(65) Carra, P.; Thole, B. T.; Altarelli, M.; Wang, X. *Phys. Rev. Lett* **1993**, *70*, 694–697.

(66) Dreiser, J. et al. *Chem. Sci* **2012**, *3*, 1024–1032.

(67) Ishikawa, N.; Sugita, M.; Wernsdorfer, W. *Angew. Chem., Int. Ed* **2005**, *44*, 2931.

Graphical TOC Entry